J. KSIAM Vol.24, No.1, 1–22, 2020 http://dx.doi.org/10.12941/jksiam.2020.24.001

LEAST-SQUARE SWITCHING PROCESS FOR ACCURATE AND EFFICIENT GRADIENT ESTIMATION ON UNSTRUCTURED GRID

SEUNGPYO SEO[1], CHANGSOO LEE[2], EUNSA KIM[2],KYEOL YUNE[2], AND CHONGAM KIM[2†]

[1]DEFENSE R&D CENTER, HANHWA CORPORATION, REPUBLIC OF KOREA
Email address: eclipse_tr@naver.com

[2]DEPARTMENT OF AEROSPACE ENGINEERING, SEOUL NATIONAL UNIVERSITY, REPUBLIC OF KOREA
Email address: chongsoo89@gmail.com, kes5885@snu.ac.kr
Email address: hwwwooo@naver.com, chongam@snu.ac.kr

ABSTRACT. An accurate and efficient gradient estimation method on unstructured grid is presented by proposing a switching process between two Least-Square methods. Diverse test cases show that the gradient estimation by Least-Square methods exhibit better characteristics compared to Green-Gauss approach. Based on the investigation, switching between the two Least-Square methods, whose merit complements each other, is pursued. The condition number of the Least-Square matrix is adopted as the switching criterion, because it shows clear correlation with the gradient error, and it can be easily calculated from the geometric information of the grid. To illustrate switching process on general grid, condition number is analyzed using stencil vectors and trigonometric relations. Then, the threshold of switching criterion is established. Finally, the capability of Switching Weighted Least-Square method is demonstrated through various two- and three-dimensional applications.

1. INTRODUCTION

Under the Finite Volume cell-centered regime, Monotonic Upwind Scheme for Conservation Laws (MUSCL) type schemes with second-order spatial discretization are extensively utilized in modern CFD solver. In the meantime, growing importance of accuracy of gradient, or derivative of flow variable, is noticeable because of its broad range of usage including solution reconstruction of MUSCL type scheme, evaluation of viscous flux and turbulent source term.

With gradual increment in complexity of geometry of flow problem, many CFD practitioners are counting on unstructured grid where automatic mesh generation greatly relieves the burden of laborious task. However, absence of organized cell-to-cell connectivity on unstructured grid brings about another challenge, that is, general way of approximating a cell-centered gradient is not applicable anymore. On the unstructured grid, two most popular approaches for obtaining estimate of gradient are method by Green-Gauss theorem and Least-Square method. However,

Received by the editors March 4 2020; Accepted March 10 2020; Published online March 25 2020.
2000 *Mathematics Subject Classification.* 93B05.
Key words and phrases. Gradient, Gradient estimation method, Least-Square method, Switching process, Condition number, Green-Gauss theorem, Unstructured grid.

† Corresponding author.

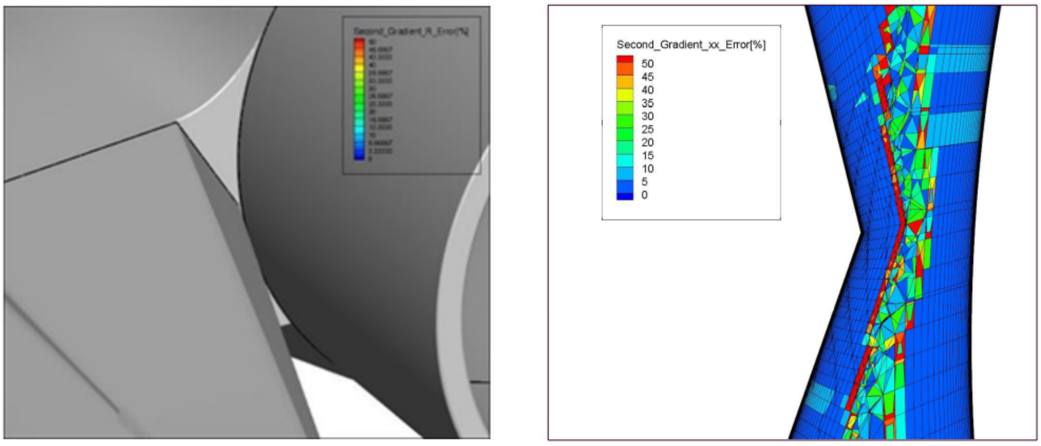

FIGURE 1. The geometry and grid where gradient accuracy is deteriorated

no consensus over the accuracy, robustness, and efficiency are made up to this day. Mavriplis [1] pointed out that Least-Square method with compact stencil (or nearest neighbor) may lead to poor gradient accuracy when applied to a cell with high aspect ratio, especially near surface curvature. Diskin *et al*. [2] and Correa *et al*. [3] made comparison between existing gradient estimations on diverse regular and irregular grids. Shima *et al.* [4] came up with an idea to mix the advantages of two popular gradient estimation methods.

Meanwhile, severe gradient accuracy degradation is detected near a narrow and complicated configuration of the aircraft, especially at the space between the tail control surface and the nozzle in Fig. 1. During the computation, breakdown of gradient accuracy causes a numerical oscillation at the region, leading to the simulation failure in the end. The full configuration of the aircraft is not presented here for security concerns.

The present research aims at proposing a gradient estimation method which is accurate and efficient on arbitrary unstructured mesh. To be specific, the goal of this work is devising a switching process between two Least-Square methods on qualitative and quantitative basis. The material in this paper is organized in the following order. Section 2 introduces the basic concept of Green-Gauss theorem and Least-Square methods investigated in this paper. Section 3 deals with comparison of results by existing gradient estimation methods via diverse test cases. Based on section 3, section 4 describes how the switching Least-Square method is developed. Section 5 shows applications of SWLSQ together with CWLSQ and EWLSQ. Lastly, Section 6 summarizes the content of this work.

2. GRADIENT ESTIMATION METHODS

2.1. **Least Square Method.** Least-Square method is a broadly used approach for approximating the solution of overdetermined system in various applications. In this case, it is utilized to estimate the gradient of a cell on unstructured grid. The overdetermined system where the

Least-Square method is applied can be derived from the first-order Taylor series expansion about the cell of interest

$$\phi_j = \phi_i + \nabla\phi_i \cdot \overrightarrow{d_{ij}}, \tag{2.1}$$

where ϕ_i and ϕ_j are flow quantities at the target cell and the neighboring cell (or stencil) respectively, and $\overrightarrow{d_{ij}}$ is a vector from the cell *i* to the stencil *j*. Furthermore, $\nabla\phi_i$ is the gradient of the target cell which stands for the rate of change of flow quantity in *x*, *y*, and *z* direction. Applying the Eq. (2.1) to all surrounding stencils, and rearranging the equations, following overdetermined system of equations is derived

$$\begin{bmatrix} \Delta x_{i1} & \Delta y_{i1} & \Delta z_{i1} \\ \Delta x_{i2} & \Delta y_{i2} & \Delta z_{i2} \\ \vdots & \vdots & \vdots \\ \Delta x_{iN} & \Delta y_{iN} & \Delta z_{iN} \end{bmatrix} \begin{bmatrix} (\partial\phi/\partial x) \\ (\partial\phi/\partial y) \\ (\partial\phi/\partial z) \end{bmatrix}_i = \begin{bmatrix} \Delta\phi_{i1} \\ \Delta\phi_{i2} \\ \vdots \\ \Delta\phi_{iN} \end{bmatrix}, \tag{2.2}$$

or

$$A\overrightarrow{x} = \overrightarrow{b}, \tag{2.3}$$

with N denoting the number of stencil and $\triangle(\cdot)_{ij} = (\cdot)_j - (\cdot)_i$. It is known [1] that Least-Square method may yield poor gradient accuracy on grid with surface curvature and high aspect ratio unless proper weighting function is accompanied by. Introducing the weighting function and multiplying A^T to both sides of Eq. (2.3), one can obtain

$$\begin{bmatrix} \sum_j^N w_{ij}\left(\Delta x_{ij}\right)^2 & \sum_j^N w_{ij}\Delta x_{ij}\Delta y_{ij} & \sum_j^N w_{ij}\Delta x_{ij}\Delta z_{ij} \\ \sum_j^N w_{ij}\Delta x_{ij}\Delta y_{ij} & \sum_j^N w_{ij}\left(\Delta y_{ij}\right)^2 & \sum_j^N w_{ij}\Delta y_{ij}\Delta z_{ij} \\ \sum_j^N w_{ij}\Delta x_{ij}\Delta z_{ij} & \sum_j^N w_{ij}\Delta y_{ij}\Delta z_{ij} & \sum_j^N w_{ij}\left(\Delta z_{ij}\right)^2 \end{bmatrix} \begin{bmatrix} (\partial\phi/\partial x)^* \\ (\partial\phi/\partial y)^* \\ (\partial\phi/\partial z)^* \end{bmatrix} = \begin{bmatrix} \sum_j^N w_{ij}\Delta x_{ij}\Delta\phi_{ij} \\ \sum_j^N w_{ij}\Delta y_{ij}\Delta\phi_{ij} \\ \sum_j^N w_{ij}\Delta z_{ij}\Delta\phi_{ij} \end{bmatrix} \tag{2.4}$$

or

$$(A^T A)\overrightarrow{x}^* = A^T\overrightarrow{b},$$

which is called the normal equation. Inversing the matrix on the left-hand side leads to

$$\overrightarrow{x}^* = (A^T A)^{-1}A^T\overrightarrow{b},$$

where $w_{ij} = 1/\left|\overrightarrow{d_{ij}}\right|^2$ is inverse square of distance between two cells, a typical weighting function, and the asterisk symbol * indicates the estimated value. Alternative ways of handling the Eq. (2.2) have also been studied by researchers, such as one implementing the Gram-Schmidt process [5, 6]. Note that the matrix on the left-hand side of the normal equation $A^T A$, or Least-Square matrix from here, is solely composed of element of distance vector $\overrightarrow{d_{ij}}$. This implies that property of Least-Square matrix, such as condition number, can be readily evaluated from the geometric information of given grid, as will be exploited in later section.

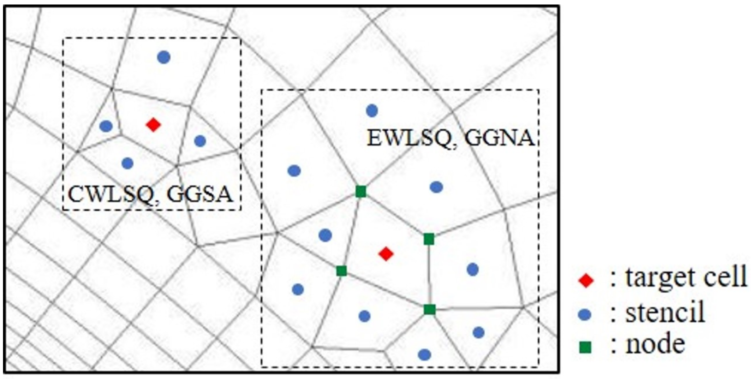

FIGURE 2. Schematic of stencil configuration of gradient estimation methods

Meanwhile, gradient by Least-Square method can be distinguished from one another by the fashion it selects the neighboring stencil. In this study, Least-Square method that chooses the compact stencil (or nearest stencil), whose face is shared with the target cell, is named Compact stencil Weighted Least-Square method (CWLSQ). In similar manner, Least-Square method that adopts extended stencil (or full augmentation), who shares cell node with the target cell, is called Extended stencil Weighted Least-Square method (EWLSQ). Fig. 2 depicts the stencil configuration of two Least-Square methods.

2.2. **Green-Gauss Theorem.** Green-Gauss theorem relates the volume integral of gradient of a scalar function ϕ to the surface integral of the ϕ, namely

$$\iiint_V \nabla\phi dV = \oiint_S \phi \cdot \overrightarrow{n} dS, \tag{2.5}$$

with V and S meaning control volume and control surface of the cell respectively. In addition, $\overrightarrow{n}$ denotes a unit normal vector pointing outward of the cell. Since the flow variable within the particular control volume is assumed to be constant in cell-centered FVM scheme, Eq. (2.5) can be expressed as

$$V\nabla\phi = \oiint_S \phi \cdot \overrightarrow{n} dS. \tag{2.6}$$

Then, surface integral of Eq. (2.6) is discretized as sum of the flow variable passing through the control surface,

$$V\nabla\phi = \sum_{k=1}^{N} \overline{\phi_k}\overrightarrow{n_k}S_k,$$

or

$$\nabla\phi = \frac{1}{V}\sum_{k=1}^{N} \overline{\phi_k}\overrightarrow{n_k}S_k, \tag{2.7}$$

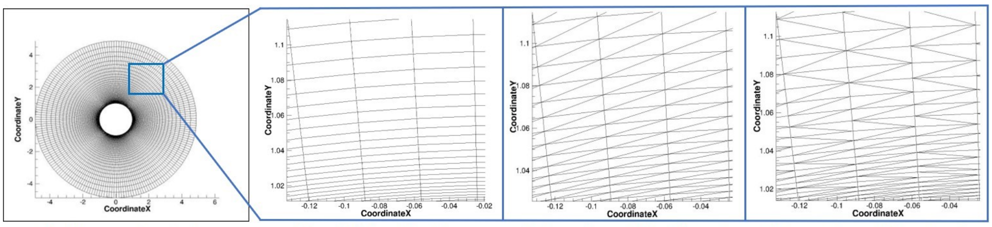

Grid around a circle **Quadrilateral grid** **Triangular grid(uniform)** **Triangular grid(random)**

FIGURE 3. Three types of grids around a circle

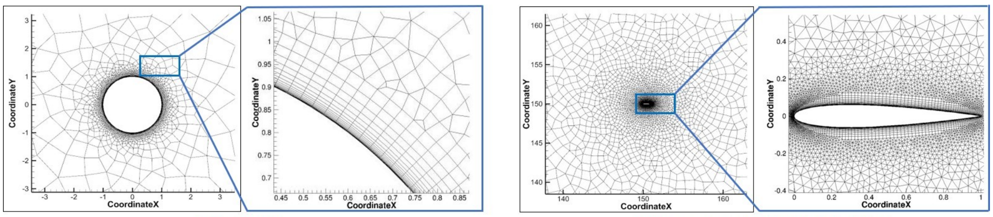

Mixed grid **Grid around a NACA0012 airfoil**

FIGURE 4. Mixed grid and grid around a NACA0012 airfoil

where $\overline{\phi_k}$, $\overrightarrow{n_k}$, and S_k refer to flow variable, unit normal vector, and face area of k-th cell face respectively. The mean flow variable at the face is only unknown which directly affects the accuracy of gradient. In this work, two branches of Green-Gauss methods are examined, Green-Gauss method using Simple Averaging (GGSA) and Node Averaging (GGNA).

GGSA approximates the cell interface value by taking an average of the left and the right flow variable of the interface, which is quite straightforward and needs little cost for application

$$\overline{\phi_k} = \frac{\phi_{left} + \phi_{right}}{2}.$$

On the other hand, the cell interface value is acquired through two steps in GGNA. Firstly, to interpolate the flow quantity at particular node of the interface, flow quantities at surrounding cell-centers are averaged, with or without inverse weight. Next, these interpolated nodal values are averaged again to estimate the cell interface value
STEP1:

$$\overline{\phi}_{node} = \frac{\sum_{j=1}^{N} w_i \phi_i}{\sum_{j=1}^{N} w_i},$$

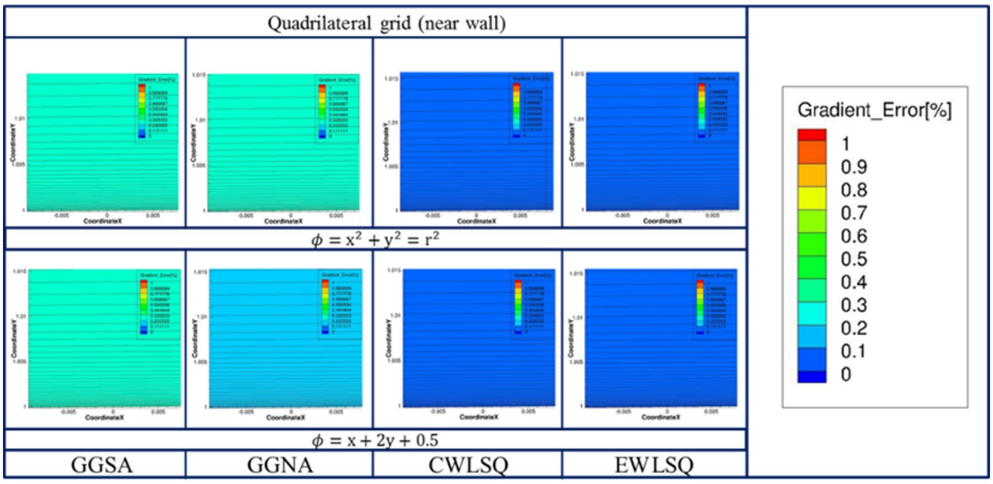

FIGURE 5. Comparison of gradient error on quadrilateral grid

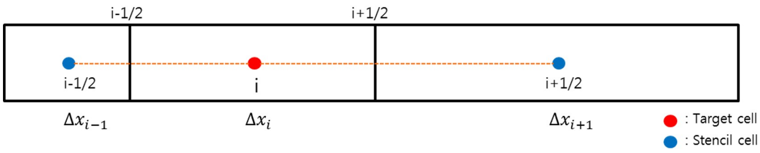

FIGURE 6. One-dimensional case with non-uniform interval

STEP2:

$$\overline{\phi_k} = \frac{\overline{\phi}_{node,1} + \overline{\phi}_{node,2} + \cdots + \overline{\phi}_{node,n}}{n},$$

Note that the capital n refers to the number of cells around the node, while lowercase n indicates the number of nodes. Same as the two Least-Square methods, the schematic of the way GGSA and GGNA refer to stencils is illustrated in Fig. 2

Although Green-Gauss methods are easy to implement with relatively little cost, these approaches possess intrinsic drawback; they cannot give exact gradient value even for a simple linear function. More details are described in the later section.

3. Analysis of Preceding Approaches

This section analyzes the accuracy of the aforementioned gradient estimation methods on diverse grid types with linear and nonlinear test function.

3.1. **Grid Type.** Five types of grids are considered; quadrilateral grid, uniformly diagonalized triangular grid, randomly diagonalized triangular grid, mixed grid, and unstructured grid around a NACA0012 airfoil. All grid types, except mixed grid and the grid around an airfoil, have things in common in that they are generated around a circle and contain cells with high aspect ratio, about 500 for maximum. This is because those regions have been a major concern of many research [1, 7, 8]. Figures 3-4 summarize figure of all grid types.

3.2. **Test Function.** In order to assess the accuracy of each gradient method, test function that can provide reference gradient value is demanded. Thus, two test functions, linear function and nonlinear function, are used as follows

$$\phi = x^2 + y^2 = r^2,$$
$$\phi = x + 2y + 0.5.$$

With the test function, gradient error is evaluated at each grid cell

$$e_i = \left| \frac{\nabla\phi_{i,exact} - \nabla\phi_{i,estimated}}{\nabla\phi_{i,exact}} \right| \times 100.$$

3.3. **Observation.** To begin with, four gradient estimation methods are compared with respect to quadrilateral grid. As stated in other studies [9, 10], Green-Gauss methods show good performance in viscous boundary layer grid, less than 1% of error, not to mention the gradient by Least-Square methods, as illustrated in Fig. 5. However, it should be noted that when it comes to the linear test function, Least-Square methods tend to produce remarkably small amount of gradient error, about $O(10^{-10})$, whereas that of Green-Gauss methods almost stay as it is regardless of grid refinement.

To inspect the properties of gradient by Green-Gauss theorem, one-dimensional grid with non-uniform spacing is employed [9] as shown in Fig. 6. Applying Eq. (2.7) results in

$$\begin{aligned} \nabla\phi_{i,GGSA} &= \frac{1}{V}\sum_{k=1}^{N} \overline{\phi_k}\overrightarrow{n_k} S_k \\ &= \frac{\phi_{i+1/2} - \phi_{i-1/2}}{\Delta x_i}. \end{aligned}$$

Substituting cell interface value with cell-centered value leads to

$$\nabla\phi_{i,GGSA} = \frac{\phi_{i+1} - \phi_{i-1}}{2\Delta x_i} \tag{3.1}$$

Then, ϕ_{i+1} and ϕ_{i-1}, obtained from Taylor series expansion, are replaced into Eq. (3.1)

$$\begin{aligned} \nabla\phi_{i,GGSA} &= \nabla\phi_i\left(\frac{1}{2} + \frac{\Delta x_{i+1} + \Delta x_{i-1}}{4\Delta x_i}\right) + \nabla^2\phi_i\left(\frac{\Delta x_{i+1} + \Delta x_{i-1}}{8} + \frac{{\Delta x_{i+1}}^2 + {\Delta x_{i-1}}^2}{16\Delta x_i}\right) + O(h^2) \\ &= \nabla\phi_i + \nabla\phi_i\left(-\frac{1}{2} + \frac{\Delta x_{i+1} + \Delta x_{i-1}}{4\Delta x_i}\right) + O(h) \end{aligned} \tag{3.2}$$

It is clear that the GGSA cannot recover the exact gradient, leaving zeroth-order as leading error term. Even though it may lead to second-order accuracy when unpractical uniform grid interval is assumed, Eq. (3.2) suggests that GGSA is inherently inconsistent method. As for GGNA, same conclusion is attained from procedures described above. Undoubtedly, two Green-Gauss

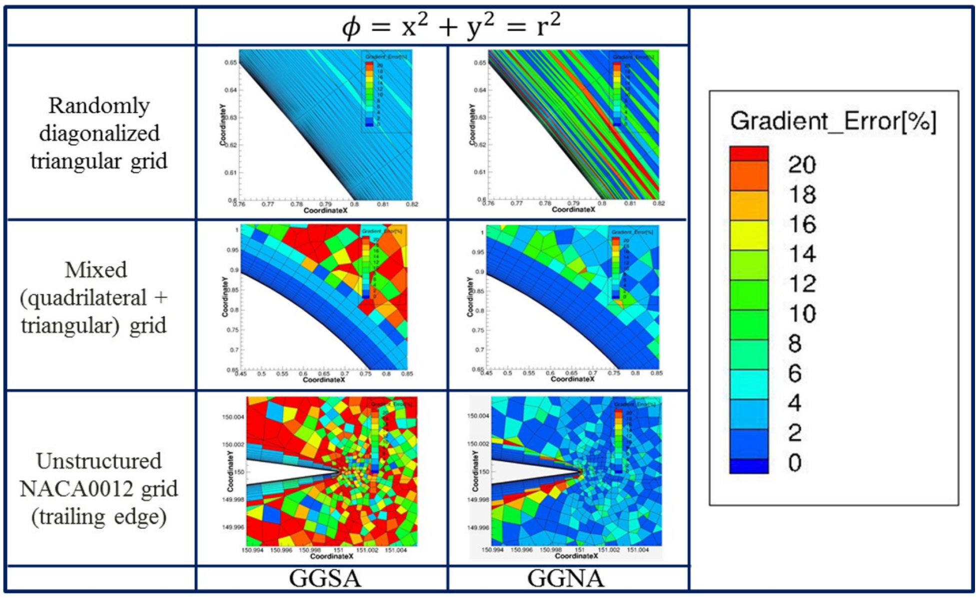

FIGURE 7. Contour of gradient error by GGSA and GGNA on other types of grid

type methods produce large gradient error on other test cases as can be found in Fig. 7. To sum up, gradient by Green-Gauss theorem should not be preferred on pragmatic grid circumstances where combination of non-uniform and diverse grid type is inevitable

In the meantime, EWLSQ outperforms CWLSQ on all kinds of grid in terms of gradient accuracy. Whereas EWLSQ shows less than 1% error on randomly diagonalized grid, for example, CWLSQ presents over 20% error near wall as shown in Fig. 8. The result from the uniform triangular grid is same as the random triangular grid that it is not shown here. Excellence in gradient accuracy of EWLSQ in overall test cases is obvious, but it should be remembered that there are cases where CWLSQ also exhibits fair gradient accuracy. Indeed, shortcoming of EWLSQ is that it necessitates about two to dozens of more stencil to estimate the gradient compared to CWLSQ, compromising computational time accordingly.

4. LEAST-SQUARE METHOD SWITCHING FUNCTION

4.1. **Motivation.** Earlier investigation shows that generally, gradient by Green-Gauss theorem is not appropriate for grid situations encountered in practical flow problems. On the other hands, EWLSQ presents overall better gradient accuracy compared to CWLSQ, paying for a number of stencils, and thus, computational cost. In addition, one should be reminded that there are cases where CWLSQ can make comparable gradient accuracy, claiming relatively little cost. Hence, this observation calls for a method where two Least-Square methods are selectively exploited under a suitable switching criterion, making use of advantage of each

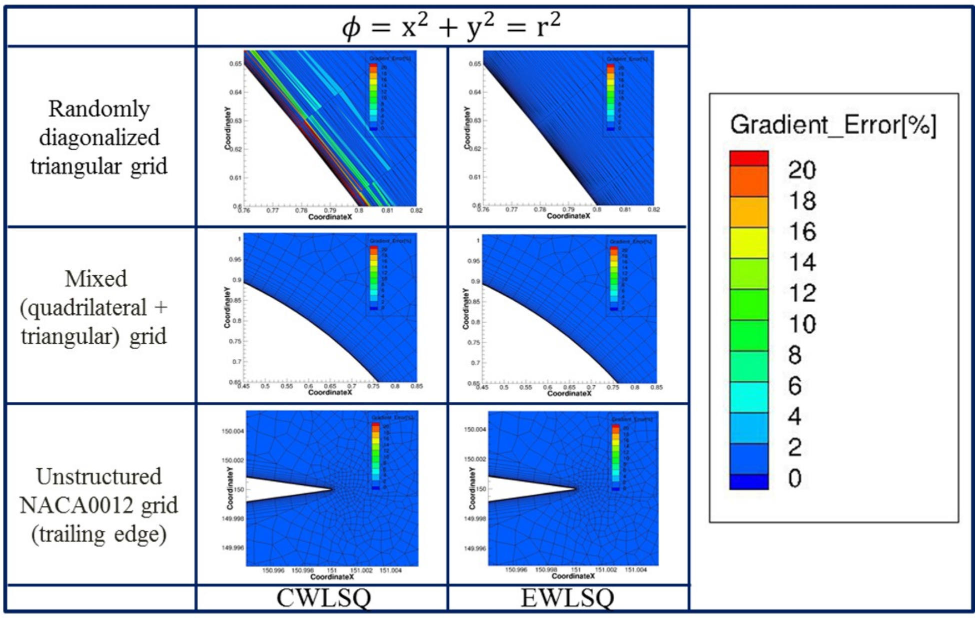

FIGURE 8. Contour of gradient error by CWLSQ and EWLSQ

method. In the meantime, to accomplish the Switching Weighted Least-Square method (or SWLSQ) on universal grid types, a consistent switching standard is mandatory.

For the first step, conventional grid quality indexes, such as aspect ratio, skewness, or area ratio, can be taken as candidates. Figure 9 describes result of gradient error versus grid quality indexes, where randomly diagonalized triangular grid and nonlinear test function are employed. However, it is evident that none of the candidates show clear link with the gradient error. From the perspective of skewness, for example, gradient error is small and plain until it soars around the skewness of about 1. Furthermore, these indexes cannot play their role properly when the target cell with favorable grid quality is surrounded by bad quality cells. Namely, even if the grid qualities of stencil are bad, since that of the target cell is satisfactory, switching method will choose CWLSQ as gradient estimation, leading to poor gradient accuracy. In short, accuracy of gradient by Least-Square methods is not only affected by the grid quality of the target cell, but also by stencil configuration around it. Therefore, switching criteria should be able to include stencil information encompassing the target cell.

4.2. **Condition number of Least-Square matrix.** In the field of linear algebra, the condition number of a matrix is used as a measure of sensitivity of the output to the change in the input. For a normal matrix A, the condition number is defined as

$$k(A) = \frac{|\lambda_{\max}(A)|}{|\lambda_{\min}(A)|},$$

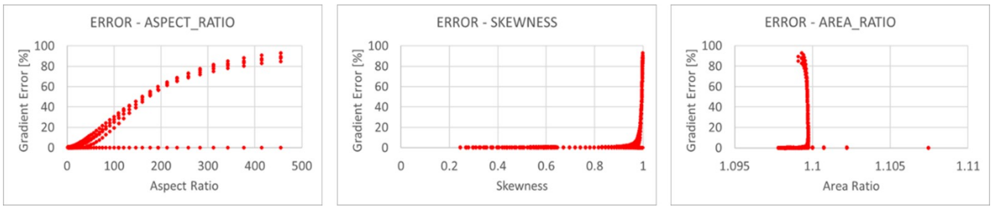

FIGURE 9. Gradient error of CWLSQ with respect to conventional grid quality criterion

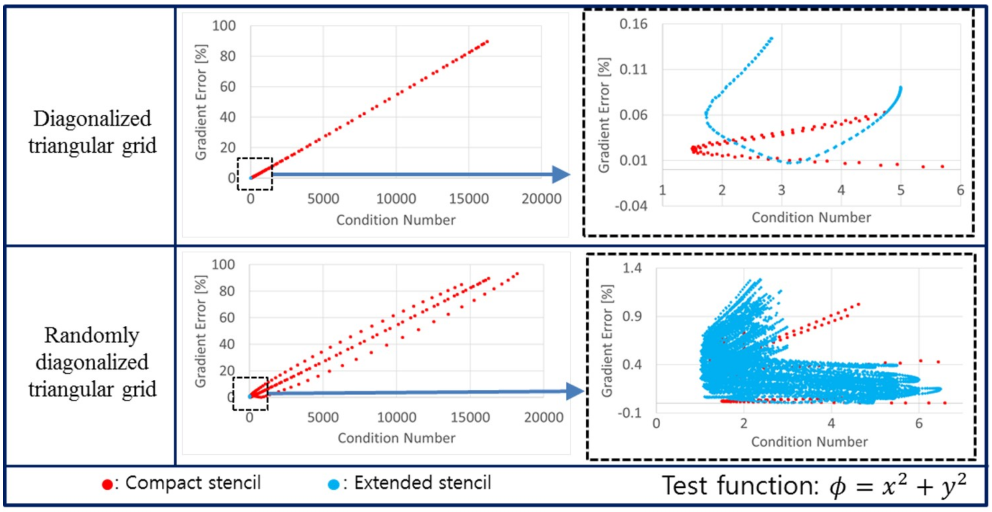

FIGURE 10. Comparison Least-Square methods regarding the condition number and the gradient error

where λ is eigenvalue of the matrix A. Revisit the Least-Square formulation in Eq. (2.4) to introduce the concept of the condition number

$$\begin{bmatrix} \sum_j^N w_{ij}(\Delta x_{ij})^2 & \sum_j^N w_{ij}\Delta x_{ij}\Delta y_{ij} & \sum_j^N w_{ij}\Delta x_{ij}\Delta z_{ij} \\ \sum_j^N w_{ij}\Delta x_{ij}\Delta y_{ij} & \sum_j^N w_{ij}(\Delta y_{ij})^2 & \sum_j^N w_{ij}\Delta x_{ij}\Delta z_{ij} \\ \sum_j^N w_{ij}\Delta x_{ij}\Delta z_{ij} & \sum_j^N w_{ij}\Delta y_{ij}\Delta z_{ij} & \sum_j^N w_{ij}(\Delta z_{ij})^2 \end{bmatrix} \begin{bmatrix} (\partial\phi/\partial x)^* \\ (\partial\phi/\partial y)^* \\ (\partial\phi/\partial z)^* \end{bmatrix}_i = \begin{bmatrix} \sum_j^N w_{ij}\Delta x_{ij}\Delta\phi_{ij} \\ \sum_j^N w_{ij}\Delta y_{ij}\Delta\phi_{ij} \\ \sum_j^N w_{ij}\Delta z_{ij}\Delta\phi_{ij} \end{bmatrix} \quad (4.1)$$

or shortly,

$$\overline{A}\overrightarrow{x}^* = A^T\overrightarrow{b}, \quad (4.2)$$

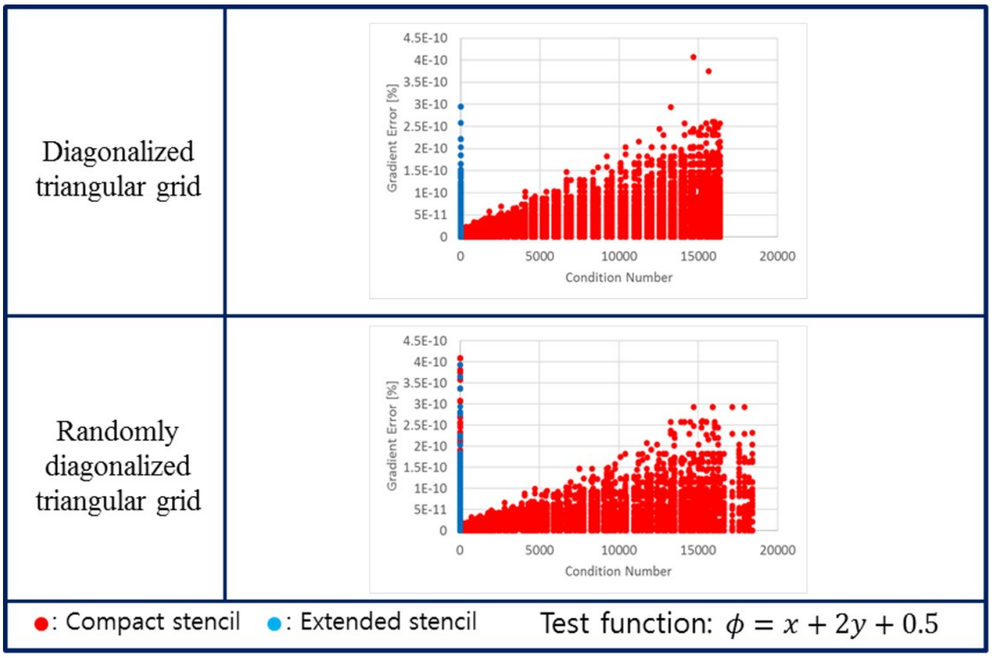

FIGURE 11. Result of two Least-Square methods about linear test function

where $\overline{A} = A^T A$ is the Least-Square matrix as stated in previous section. That is, the condition number of Least-Square matrix $k(\overline{A})$ informs how the estimated gradient $\overrightarrow{x}^*$ would respond to a small change in $A^T\overrightarrow{b}$.

Consider a case where CWLSQ and EWLSQ shows stark difference; two triangular grid types as depicted in Fig. 10. In both cases, it is clear that the gradient error of CWLSQ gradually increases in proportion to the Least-Square matrix condition number, while those of EWLSQ are found to be small and clustered around 0. The rationale behind the correlation of gradient error and condition number will be handled in next section.

Meanwhile, Eq. (4.2) can be cast into following form with slight modification on right-hand side

$$\left(A^T A\right) \overrightarrow{x}^* = \sum_{j=1}^{N} w_{ij} \overrightarrow{d}_{ij} \Delta \overrightarrow{\phi}_{ij}. \tag{4.3}$$

Here, one should be reminded that, originally, Eq. (4.3) holds second-order truncation error, which is neglected for first-order Taylor series expansion in Eq. (2.1). Namely

$$\left(A^T A\right) \overrightarrow{x}^* = \sum_{j=1}^{N} w_{ij} \overrightarrow{d}_{ij} \Delta \overrightarrow{\phi}_{ij} + O\left(h^2\right).$$

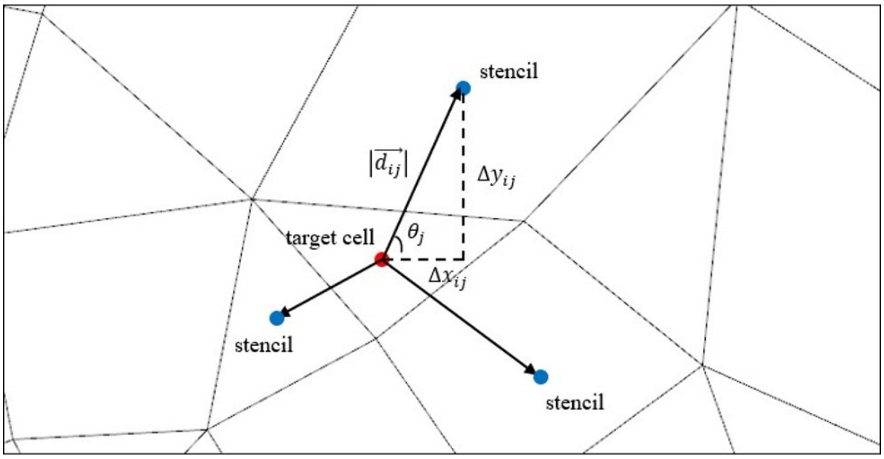

FIGURE 12. An example of stencil vectors around the target cell

From the condition number point of view, the truncation error can be interpreted as a small perturbation to input of Least-Square system. Therefore, for an ill-conditioned system, this truncation error is potential source of error, which deteriorates the gradient accuracy. On the contrary, provided that the truncation error from Least-Square formulation is sufficiently low, it barely damages the gradient accuracy even for high condition number. As shown in Fig. 11, even if CWLSQ yields condition number as high as 15000, gradient error is just bounded under $O(10^{-10})$.

In summary, unlike the conventional grid quality indexes, condition number of Least-Square matrix has clear connection with gradient error. In addition, as in the Eq. (4.1), the Least-Square matrix is made up of element of distance vector, which is entirely geometric information of given grid. Thus, the condition number of each cell can be pre-computed and stored before numerical iterations.

4.3. **Behavior of condition number of CWLSQ and EWLSQ.** Earlier example presents the condition number is closely concerned to the gradient error of Least-Square methods, indicating that the condition number can be a good switching criterion. Remaining questions are; why CWLSQ leads to large condition number with poor gradient accuracy, and what's the suitable threshold of condition number for two Least-Square methods to be effectively alternated.

For further analysis, consider a two-dimensional case whose Least-Square matrix size is 2×2

$$\overline{A} = \begin{bmatrix} \sum_j^N w_{ij}(\Delta x_{ij})^2 & \sum_j^N w_{ij}\Delta x_{ij}\Delta y_{ij} \\ \sum_j^N w_{ij}\Delta x_{ij}\Delta y_{ij} & \sum_j^N w_{ij}(\Delta y_{ij})^2 \end{bmatrix} = \begin{bmatrix} a & b \\ c & d \end{bmatrix}, \tag{4.4}$$

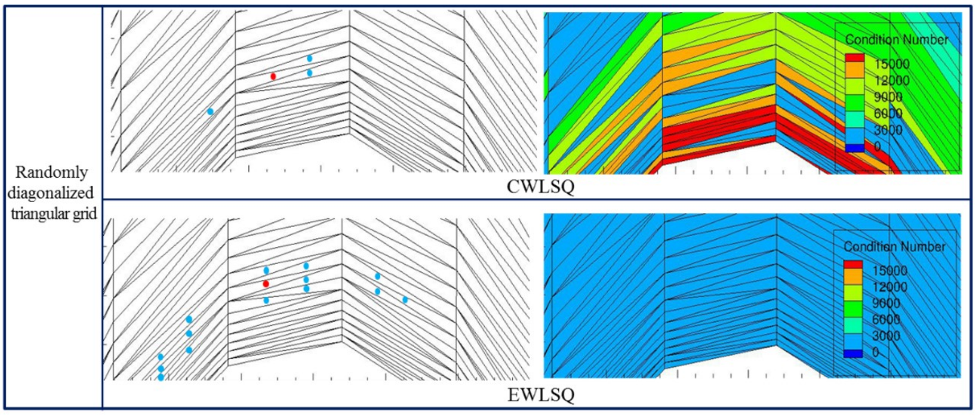

$$k(A) = \frac{N + \sqrt{N+p}}{N - \sqrt{N+p}}$$

	N	p	$k(A)$	Error [%]
CWLSQ	3	2.9995	**14434**	**68**
EWLSQ	14	9.9952	**6**	**0.14**

FIGURE 13. An example of stencil vectors around the target cell

where components of the matrix are replaced with a, b, c, and d for simplicity. By definition of the condition number

$$k(\overline{A}) = \frac{|\lambda_{\max}|}{|\lambda_{\min}|} = \frac{(a+d) + \sqrt{(a-d)^2 + 4bc}}{(a+d) - \sqrt{(a-d)^2 + 4bc}}. \tag{4.5}$$

Then, trigonometric function and its identities are introduced to Eq. (4.5) for better understanding, using a concept of stencil vectors illustrated in Fig. 12.

For example, $a + d$ in Eq. (4.5) can be exchanged with simpler and informative expression N, which refers to the number of the stencil used for gradient estimation

$$a + d = \sum_{j=1}^{N} w_{ij}(\Delta x_{ij}^2 + \Delta y_{ij}^2) = N.$$

Likewise, every term in Eq. (4.5) are replaced as follows

$$\begin{aligned} a - d &= \sum_{j=1}^{N} w_{ij}({\Delta x_{ij}}^2 - {\Delta y_{ij}}^2) \\ &= \sum_{j=1}^{N} \frac{\left(\left|\overrightarrow{d_{ij}}\right|^2 \cos^2\theta_j - \left|\overrightarrow{d_{ij}}\right|^2 \sin^2\theta_j\right)}{\left|\overrightarrow{d_{ij}}\right|^2} = \sum_{j=1}^{N} \cos 2\theta_j, \end{aligned}$$

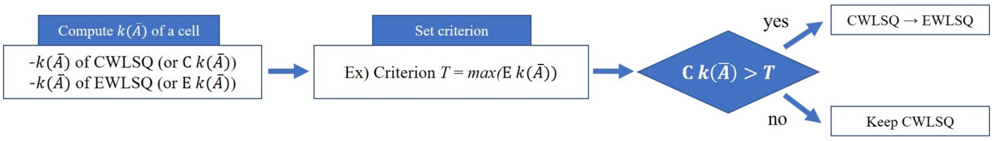

FIGURE 14. Switching process between two Least-Square methods

$$
\begin{aligned}
4bc &= 4\sum_{j=1}^{N} w_{ij}\Delta x_{ij}\Delta y_{ij} \sum_{j=1}^{N} w_{ij}\Delta x_{ij}\Delta y_{ij} \\
&= 4\sum_{j=1}^{N} \cos\theta_j \sin\theta_j \sum_{j=1}^{N} \cos\theta_j \sin\theta_j = \left(\sum_{j=1}^{N} \sin 2\theta_j\right)^2 .
\end{aligned}
$$

Finally, Eq. (4.5) can be rewritten to obtain new expression about the condition number

$$
\begin{aligned}
k(\overline{A}) &= \frac{(a+d) + \sqrt{(a-d)^2 + 4bc}}{(a+d) - \sqrt{(a-d)^2 + 4bc}} \\
&= \frac{N + \sqrt{N+p}}{N - \sqrt{N+p}},
\end{aligned}
$$

where p is a function of angles described by stencil vectors. For two-dimensional quadrilateral grid, where a target cell has four stencils, p is represented as follows

$$
p = 2[\cos 2(\theta_1 - \theta_2) + \cos 2(\theta_1 - \theta_3) + \cdots + \cos 2(\theta_3 - \theta_4)].
$$

When it comes EWLSQ which takes about ten times more stencils than CWLSQ in three-dimensional case, the condition number can stay low because relatively large N in denominator keeps the condition number from being amplified. In contrast, CWLSQ is vulnerable to dramatic change of condition number, and consequently, it brings about undesirably large gradient error. The test case of Fig. 13 demonstrates the different behavior of CWLSQ and EWLSQ. About four times greater number of stencils of EWLSQ prevents the condition number from exponential increment, while CWLSQ fails to do so.

Thanks to large number of stencils, EWLSQ can achieve lower condition number compared CWLSQ regardless of grid type. Therefore, one might propose the maximum condition number of EWLSQ as the threshold of switching value. That is, a grid cell whose condition number of CWLSQ exceeds the maximum condition number of EWLSQ should adopt a wider range of stencil before moving onto actual flow computation. However, it will be shown that setting the maximum condition number of EWLSQ as the limit of conversion may display advantages in the grid around a simple geometry, but this standard is susceptible to overshoot of condition number found in complex applications. Some may suggest certain fixed value as a criterion, which is simple and convenient, but certain magnitude of number is not capable of handling the condition number disparity arise from various geometry and different dimensions. Another possible candidate for switching value is mean condition number of EWLSQ. In the following

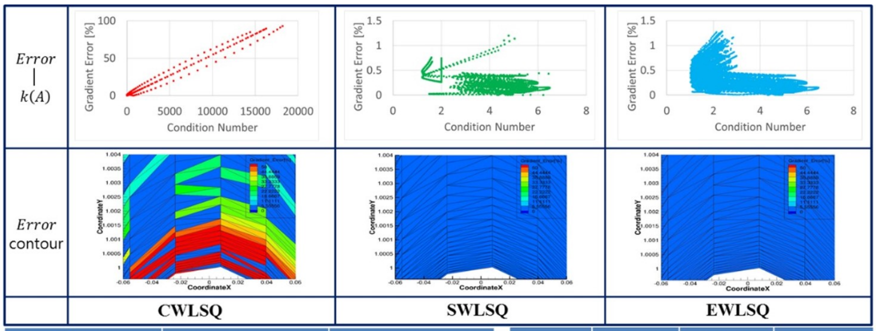

Criterion	Max $E\ k(A) = 7$	Avg $E\ k(A) = 3.6$
Number of switched cell	11797	13703
switched / total cell ratio [%]	32.2	37.4

	CWLSQ	SWLSQ	EWLSQ
Max $k(A)$	18194	7	7
Max Error [%]	93.06	1.28	1.28

FIGURE 15. Comparison of three Least-Square methods on 2D triangular grid

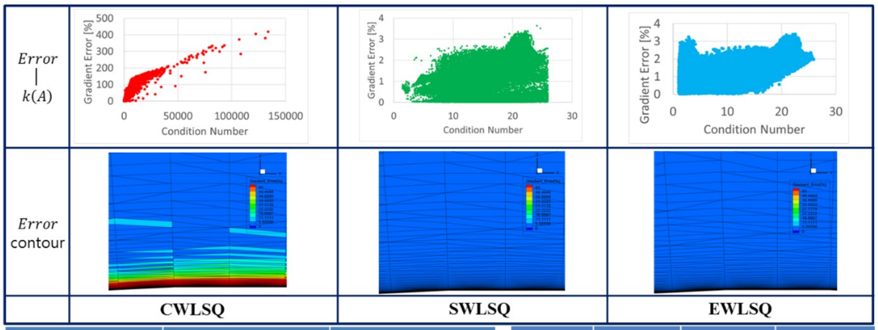

Criterion	Max $E\ k(A) = 26$	Avg $E\ k(A) = 11.0$
Number of switched cell	858594	942607
switched / total cell ratio [%]	49.6	54.4

	CWLSQ	SWLSQ	EWLSQ
Max $k(A)$	133788	26	26
Max Error [%]	418.73	3.63	3.40

FIGURE 16. Comparison of three Least-Square methods on 3D tetrahedral grid

section, maximum condition number and average condition number of EWLSQ are explored simultaneously for switching value.

4.4. **Simple Demonstration.** Capability of Switching Weighted Least-Square method (SWLSQ) and two Least-Square methods are compared in simple two- and three-dimensional example. Henceforth, SWLSQ stands for a type of Least-Square method switching between CWLSQ and EWLSQ based on certain criterion.

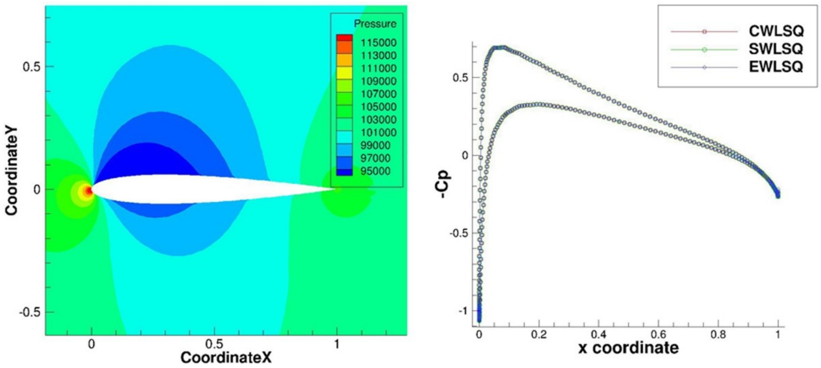

Criterion	Max $E\,k(A) = 4.01$
Number of switched cell	53
switched / total cell ratio [%]	0.24

LSQ method	CWLSQ	SWLSQ	EWLSQ
Max $k(A)$	9.3	4.01	4.01
Computation time [sec]	605	610	745

FIGURE 17. Comparison of three Least-Square methods on NACA0012 airfoil

Figure 15 describes the result of three Least-Square methods applied to randomly diagonalized triangular grid around a circle with nonlinear test function. The plot and the contour described in Fig. 15 are based on maximum condition number. As for the maximum condition number, about 32% of cell are switched from CWLSQ to EWLSQ, reducing the gradient error as low as EWLSQ. With the average condition number, approximately 5% more cells are converted from CWLSQ to EWLSQ. This result may give an impression that the maximum condition number is a more effective switching criterion for SWLSQ. However, shortcoming of the maximum condition number is revealed in more complex practices. Similar observation is found in random tetrahedral grid around a sphere as in Fig. 16. When CWLSQ is used alone, the gradient error skyrockets over 400%, but the switching mechanism successfully helps SWLSQ to restore the gradient accuracy.

5. APPLICATION

5.1. **Two-dimensional NACA0012 airfoil.** Firstly, flow over a two-dimensional NACA0012 airfoil is examined. A brief explanation about the case is listed in Table 1. Thanks to decent grid quality around the NACA0012 airfoil, CWLSQ shows mild level of condition number in entire flow space. Therefore, SWLSQ does not need to employ large number of EWLSQ stencil, and thus, about 1% of cell were switched from CWLSQ to EWLSQ. Hence, as depicted in Fig. 17, result by three Least-Square method provides almost same pressure coefficient. However, one should note that SWLSQ can save about 18% of computation time compared to EWLSQ.

5.2. **Three-dimensional wing-body configuration.** Three-dimensional wing-body configuration, or common research model (CRM), is another commonly used verification model. First of all, it should be mentioned that SWLSQ fails to compute the simulation when maximum condition number of EWLSQ is used as the threshold for switching process. This is because few cells with exceptionally large EWLSQ condition number are detected, and these cells make the criterion too loose to control the switching process. In general, this kind of cells inhabit near boundary cells where abnormal stencil distribution is inevitable. As a result, only an insufficient number of cells are switched, and SWLSQ fails the simulation. Therefore, from now on, mean EWLSQ condition number is exploited for stability issue.

As described in Fig. 14, one should check the condition number of two Least-Square methods beforehand. As for the CRM geometry, Fig. 18 shows that grid near the trailing edge of the wing is potential source of trouble, with high CWLSQ condition number. While CWLSQ alone produces maximum gradient error of about 260%, SWLSQ with average condition number enables the gradient accuracy to recover to EWLSQ level.

A brief description about the case is shown in Table 2. As expected from bad condition number at the wing, CWLSQ fails to solve this flow problem. In contrast, SWLSQ not only reduces computational time by 10% from EWLSQ, but also predict lift and drag coefficient as accurately as EWLSQ (Table 3), giving almost same pressure contour in Fig. 19.

TABLE 1. Summary of the flow simulation over NACA0012 airfoil

Simulation Information	**Value**
Mach Number	0.5
Angle of Attack	1.25
Reynolds Number	1.1×10^7
Flow Type	Turbulent Flow
Turbulence model	Menter's k-w SST
Convective flux	RoeM [11]
Time Integration Method	Implicit Euler
Linear Algebra Method	LU-SGS

TABLE 2. Summary of the flow simulation over CRM

Simulation Information	**Value**
Mach Number	0.85
Angle of Attack	2.3
Reynolds Number	5.1×10^6
Flow Type	Turbulent Flow
Turbulence model	Menter's k-w SST
Convective flux	AUSMPW+ [12]
Time Integration Method	Implicit Euler
Linear Algebra Method	GMRES

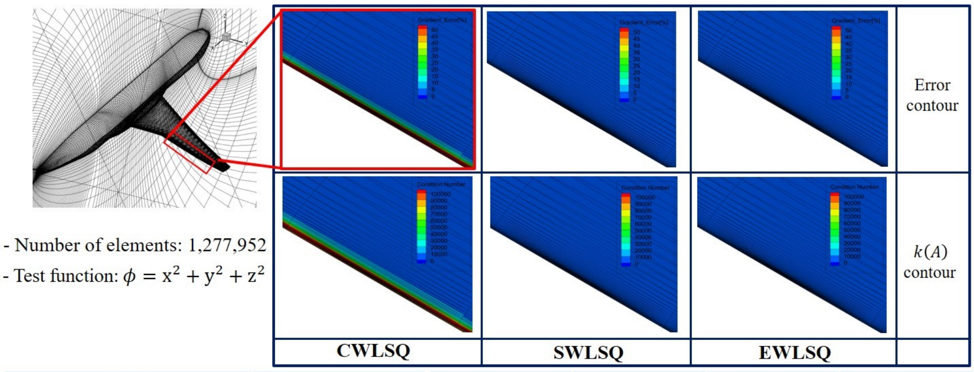

Criterion	$Avg\,E\,k(\bar{A}) = 10.2$
Number of switched cell	285612
switched / total cell ratio [%]	22.3

	CWLSQ	SWLSQ	EWLSQ
Max $k(\bar{A})$	778171	1247	1247
Max Error [%]	261.87	9.6	7.8

FIGURE 18. Comparison of three Least-Square methods with test function on CRM

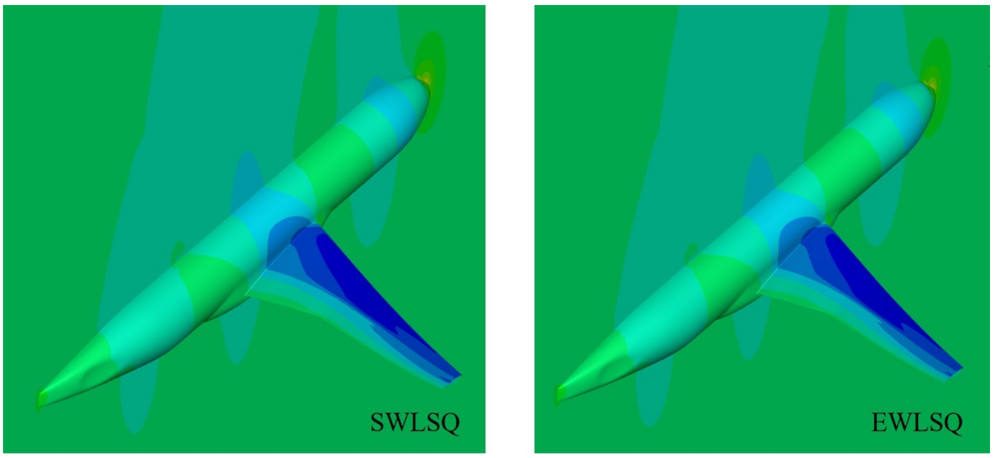

FIGURE 19. Comparison of pressure contour by two Least-Square methods

5.3. **Three-dimensional modern fighter configuration.** To present the switching on more practical application, a modern fighter configuration is considered. It is mentioned here that details of computation, including full configuration, result of aerodynamic coefficients are not disclosed for security reasons. As in the CRM case, the condition number of SWLSQ is measured against other two Least-Square methods. Then aerodynamic coefficients as well as computation time is compared to show excellence of SWLSQ.

In general, second gradient at a cell is obtained by applying the gradient estimation methods twice in a row. Thus, it is natural to guess that good first-gradient (or first-derivative) accuracy

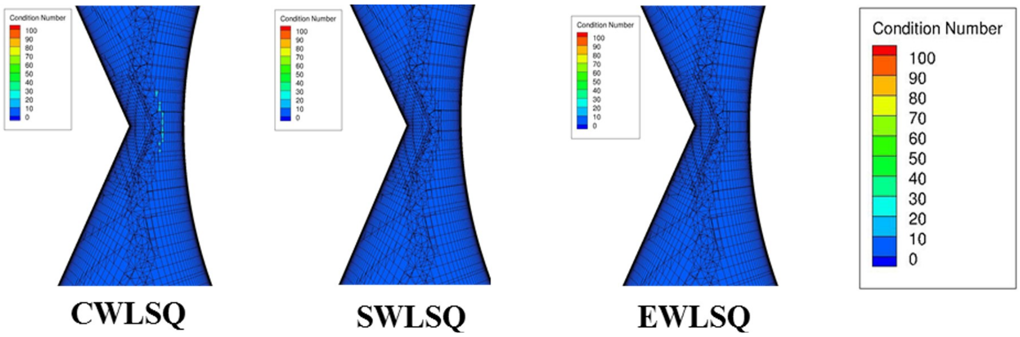

FIGURE 20. Condition number by three Least-Square methods at the problematic region

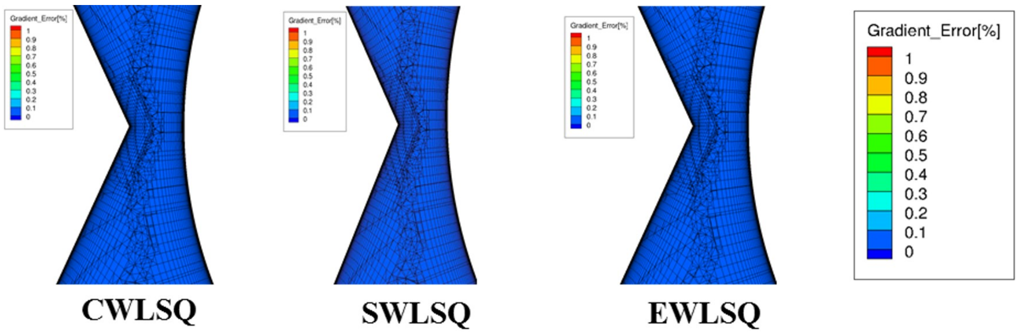

FIGURE 21. First gradient error by three Least-Square methods at the problematic region

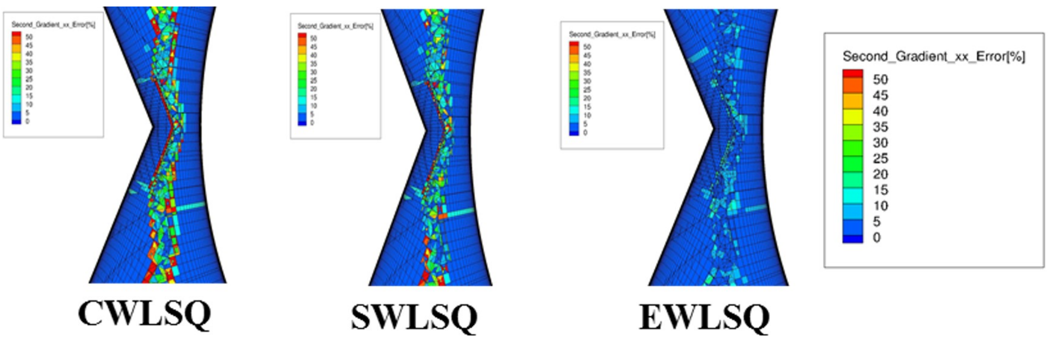

FIGURE 22. Second gradient error by three Least-Square methods at the problematic region

would lead to fair second-gradient (or second-derivative) accuracy. However, good condition number (Fig. 20) and first-gradient accuracy (Fig. 21) of CWLSQ do not generate fine second-gradient accuracy, as seen in Fig. 22. While it is true that SWLSQ somewhat succeeds in helping second-gradient accuracy to be improved in the problematic space, this suggests that additional research to figure out the relation between the condition number and the second gradient is needed.

Numerical schemes and relevant flow conditions of this case are listed in Table 4. As predicted by the poor second gradient accuracy, CWLSQ fails to compute this flow problem. In Fig. 23, it is confirmed that SWLSQ converges to a value within 1% of range from coefficients of EWLSQ. Meanwhile, efficiency of SWLSQ is well presented via comparison of computation time in Table 5, where switching process ended up with saving about 32% of computation time.

TABLE 3. Aerodynamic coefficients and computation time of SWLSQ and EWLSQ in CRM case

Least-Square method	**SWLSQ**	**EWLSQ**	**Error [%]**
C_L	0.5042	0.5036	0.12
C_D	0.0288	0.0287	0.35
Computation Time [sec]	37810	41613	-

TABLE 4. Summary of the flow simulation over the modern fighter

Simulation Information	**Value**
Mach Number	Transonic region
Angle of Attack	high angle of attack
Reynolds Number	$O(10^6)$
Flow Type	Turbulent Flow
Turbulence model	Menter's k-w SST
Convective flux	RoeM [11]
Time Integration Method	Implicit Euler
Linear Algebra Method	GMRES

TABLE 5. Summary of the flow simulation over the modern fighter

Least-Square method	**SWLSQ**	**EWLSQ**
$C_L$error [%]	0.64	-
$C_D$error [%]	0.60	-
Computation Time [hr]	68.18	99.59

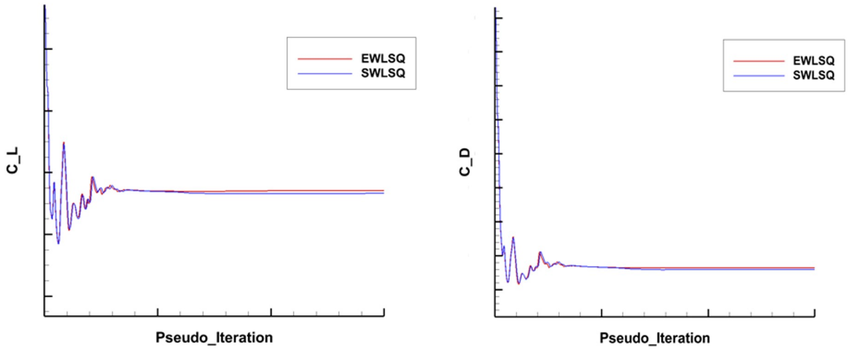

FIGURE 23. Convergence history of Least-Square methods about aerodynamic coefficients

6. CONCLUSION

A switching Least-Square method is proposed by combining the advantages of CWLSQ and EWLSQ. Firstly, four gradient estimation methods, two by Green-Gauss theorem and others by Least-Square methods, are investigated on various test cases, leading to following conclusion: 1. Gradient by Green-Gauss theorem is basically inconsistent and should not be preferred in general applications; 2. EWLSQ can give best gradient accuracy among the estimation methods, but it grabs large number of stencils; 3. On particular instances, CWLSQ which claims less number of stencils, can give as accurate result as EWLSQ with corresponding less computation time.

Based on observation, an idea of switching between CWLSQ and EWLSQ is devised. For consistent implementation on general types of grid, the condition number of the Least-Square system, which shows close correlation with the gradient error, is chosen as the switching criterion. Another merit of using the condition number is that it requires least amount of grid information. Trigonometric functions and relations are applied to Least-Square matrix to show the behavior of CWLSQ and EWLSQ, revealing the reason why EWLSQ tends to have low condition number in general cases. Then, average condition number of the EWLSQ is adopted as a threshold of the criterion.

Finally, the accuracy and efficiency of SWLSQ is compared with EWLSQ from simple to complex applications, where CWLSQ mostly fails the computation. With respect to the accuracy, it is shown that SWLSQ can produce as accurate result as EWLSQ on complicated geometry. What's more SWLSQ shows its strength regarding the efficiency in that it saves computation time about 10 to 30% depending on the flow problem. Meanwhile, as for the modern fighter configuration, it was found that accurate first-gradient does not guarantee the accuracy of second-gradient, imparting the necessity of further research.

ACKNOWLEDGEMENT

Authors would like to thank the Institute of Engineering Research at Seoul National University for providing research facilities for this work. This research was in part supported by the Institute of Advanced Aerospace Technology.

REFERENCES

[1] D. J. Mavriplis, *Revisiting the Least-Square Procedure for Gradient Reconstruction on Unstructured Meshes*, AIAA Paper 2003-3986, 18^{th} AIAA CFD conference, Orlando, Florida 2003.

[2] B. Diskin, J. L. Thomas, *Comparison of Node-Centered and Cell-Centered Unstructured Finite Volume Discretization: Inviscid Fluxes*, AIAA Journal, **4** (2011), 836-854.

[3] C. D. Correa, R. Hero, K. Ma, *A Comparison of Gradient Estimation Methods for Volume Rendering on Unstructured Meshes*, IEEE Transactions on visualization and computer graphics, **3** (2011), 305-319.

[4] E. Shima, K. Kitamura, K. Fujimoto, *New Gradient Calculation Method for MUSCL Type CFD Schemes in Arbitrary Polyhedra*, AIAA Paper 2010-1081, 48th AIAA Aerospace Sciences Meeting, Orlando, Florida 2010.

[5] W. K. Anderson, D. L. Bonhaus, *An Implicit Upwind Algorithm for Computing Turbulent Flows on Unstructured Grids*, Computers & Fluids, **1** (1994), 1-21.

[6] A. Haselbacher, J. Blazek, *On the Accurate and Efficient Discretization of the Navier-Stokes Equations on Mixed Grids*, AIAA Journal, **11** (2000), 2094-2102.

[7] N. Petrovskaya, *The Accuracy of Least-Square Approximation on Highly Stretched Meshes*, International Journal of Computational Methods, **3** (2008), 449-462.

[8] B. Diskin, J. L. Thomas, *Accuracy of Gradient Reconstruction on Grids with High Aspect Ratio*, NIA 2008-12, National Inst. Of Aerospace Dept, Hampton, Virginia 2008.

[9] E. Sozer, C. Brehm, C. Kiris, *Gradient Calculation Methods on Arbitrary Polyhedral Unstructured Meshes for Cell-Centered CFD Solvers*, AIAA 2014-1440, SciTech2014, National Harbor, Maryland 2014.

[10] E. Shima, K.Kitamura, T. Haga, *Green-Gauss/Weighted Least-Squares Hybrid Gradient Reconstruction for Arbitrary Polyhedra Unstructured Grids*, AIAA Journal, **11** (2013), 2740-2747.

[11] S. Kim, C. Kim, O. Rho, S. K. Hong, *Cures for the Shock Instability: Development of a Shock-Stable Roe Scheme*, Journal of Computational Physics, **2** (2003), 342-374.

[12] K. H. Kim, C. Kim, O. Rho, *Methods for the Accurate Computations of Hypersonic Flows*, Journal of Computational Physics, **1** (2001), 38-80.

[13] S. Seo, *Design of Least-Square Switching Function for Accurate and Efficient Gradient Estimation on Unstructured Grid*, Department of Mechanical and Aerospace Engineering, Seoul National University, Seoul, Republic of Korea, 2019.

[14] J. D. Anderson, *Fundamentals of Aerodynamics 5th ed*, McGraw-Hill, New York, 2011.

[15] K. A. Hoffmann, S.T. Chiang, *Computational Fluid Dynamics 4th ed*, Engineering Education System, Kansas, 2000.

[16] E. F. Toro, *Riemann Solvers and Numerical Methods for Fluid Dynamics 3rd ed*, Springer, Berlin, 2009

[17] R. J. Leveque, *Finite Volume Methods for Hyperbolic Problems 1st ed*, Cambridge University Press, Cambridge, 2002.

[18] G. H. Golub, C. F. Van Loan, *Matrix Computations 4th ed*, The Johns Hopkins University Press, Baltimore, 2013.